Talanta 208 (2020) 120469

Contents lists available at ScienceDirect

Talanta

journal homepage: www.elsevier.com/locate/talanta

Rapid *in situ* analysis of L-histidine and α-lactose in dietary supplements by fingerprint peaks using terahertz frequency-domain spectroscopy

Yongmei Wang[a], Zongshan Zhao[a,*], Jianyuan Qin[b], Huan Liu[a], Aifeng Liu[a], Mengmeng Xu[a]

[a] CAS Key Laboratory of Biobased Materials, Qingdao Institute of Bioenergy and Bioprocess Technology, Chinese Academy of Sciences, Qingdao, 266101, China
[b] Centre for Terahertz Research, China Jiliang University, Hangzhou, 310018, China

ARTICLE INFO

Keywords:
Terahertz spectroscopy
In situ
Rapid analysis
L-histidine
α-Lactose
Dietary supplement

ABSTRACT

A simple, green and nondestructive method based on terahertz fingerprint peaks has been developed for rapid *in situ* analysis of L-histidine and α-lactose in dietary supplements. Fingerprint absorption peaks of L-histidine and α-lactose located at 0.77 and 0.53 THz could be directly used for identification and quantitation of these analytes in commercial dietary supplements. Compared with the partial least squares regression model (PLSR), the linear least squares regression (LLSR) method based on peak areas presented better performance, with the linear correlation coefficients of 0.9899 and 0.9910 for L-histidine and α-lactose, respectively. Furthermore, analysis time per sample can be shortened to less than 1 min due to the narrower spectral acquisition region. The accuracies were 94.8–110% and 98.9–110%, comparable to those of ion chromatography for L-histidine and high-performance liquid chromatography for α-lactose. The results presented great potential of the developed method for rapid *in situ* analysis of nutrients in dietary supplements.

1. Introduction

Dietary supplements, one kind of manufactured product, often contain one or more nutrients such as vitamins, amino acids, minerals and other substances offering beneficial biological effects [1,2]. Owing to the increasing consumer health-consciousness and a tendency for self-medication, there has been tremendous growth in sales of these products [3,4]. Currently, multitudinous new products, including local and unrecognized varieties, are continuously launched into pharmacies, health food stores, and supermarkets [5,6]. Correspondingly, this often leads to quality control problems, with the appearance of many counterfeits and/or low-quality dietary supplements [7], and quality inspection on the production line is necessary to satisfy production requirements and guarantee food safety for consumers [8].

As essential nutrients in dietary supplements, some effective methods have been developed and used for amino acids and lactose in food matrices [9,10]. The most widespread methods are chromatography and mass spectrometry because of their superior sensitivity and selectivity [11]. In view of the demand for routine analysis of large amounts of samples, developing rapid and nondestructive methods is still quite necessary as conventional strategies of chromatography and mass spectrometry are time-consuming and destructive to the specimens [12]. In recent years, spectroscopic methods [13–15], such as Raman spectroscopy, near-infrared (NIR) spectroscopy and infrared (IR) spectroscopy, have also been preliminarily used for analyzing these substances, mainly because of their nondestructive testing ability and generally simple sample pretreatment [16,17]. Nevertheless, each detection method has its own advantages and disadvantages [18,19], which makes it difficult to satisfy all of the requirements for food detection by one certain technique, owing to the diversity and complexity of food matrices. Therefore, in order to satisfy the pressing demands of food safety, more potential techniques must be pioneered and developed for chemical composition detection.

Terahertz (THz) spectroscopy, locating between the microwave and infrared regions [20–22], offers characteristics of high penetrability, fingerprint spectra and low ionization energy [23,24]. Since the fingerprint vibrational/rotational frequency of most chemical and biological molecules lies in the THz region [23,25], this method has been successfully applied for the analysis of a large variety of samples, such as pesticide residues in food matrices, amino acids in foxtail millet substrates, bovine serum albumin thin-films/solutions, and new gene encoding proteins, among others [8,20,21,23,27]. Combined with chemometrics, THz spectroscopy has been proven to represent a potential strategy for quantitative and qualitative analysis of these chemical and biological molecules [23,27]. Due to its low, nonionizing energy, THz spectroscopy offers advantages of noninvasive and

* Corresponding author.
E-mail addresses: wang_ym@qibebt.ac.cn (Y. Wang), zhaozs@qibebt.ac.cn (Z. Zhao), qinjianyuan44@163.com (J. Qin), liuhuan@qibebt.ac.cn (H. Liu), liuaf@qibebt.ac.cn (A. Liu), xumm@qibebt.ac.cn (M. Xu).

https://doi.org/10.1016/j.talanta.2019.120469
Received 8 August 2019; Received in revised form 9 October 2019; Accepted 10 October 2019
Available online 11 October 2019
0039-9140/

nondestructive sensing to easily distinguish analytes from matrices for *in situ* detection [28,29]. Moreover, compared to traditional strategies, it can directly penetrate samples with or without sample pretreatment steps, which has promoted its great applicability in rapid testing [26]. Nevertheless, as far as we know, few researchers have referred to *in situ* detection of particular molecules in chemical and biological samples.

Herein, a method based on THz fingerprint peaks has been developed for *in situ* detection of L-histidine and α-lactose in dietary supplements using THz frequency-domain spectroscopy (THz-FDS). The fingerprint absorption peaks of L-histidine and α-lactose have been identified from their standard substances and then used for further quantitative analysis. The performances of partial least squares regression model (PLSR) and linear least squares regression (LLSR) chemometrics methods have been compared with respect to analyzing these two chemicals in food matrices. Additionally, the validation of the methods has also been evaluated by comparison with ion chromatography (IC) for L-histidine and high-performance liquid chromatography (HPLC) for α-lactose in dietary supplements.

2. Materials and methods

2.1. Materials and chemicals

L-histidine and α-lactose used in this paper were respectively purchased from Aladdin Reagent Co., Ltd. (Shanghai, China) and Tianjin Zhiyuan Reagent Co., Ltd. (Tianjin, China) with the purities of 99.9% and 99.5%. Polyethylene (PE) powder was supplied by Sigma-Aldrich (Beijing, China) with 40–48 μm particle size. Corn starch was purchased from Sinopharm Reagent Co., Ltd. (Beijing, China) with purity of 99.9%. Two kinds of dietary supplements (A and B) were purchased from the JD.com global online shopping site, and the major chemical compositions are given in Table 1. These two samples are the most common commercially available brands that we could collect in that period. L-histidine, α-lactose and PE powder were ground to proper sizes with a mortar and dried at 60 °C for 24 h. All chemical reagents used in the study were of analytical grade.

2.2. Sample preparation

To recognize THz fingerprint spectra of L-histidine and α-lactose, their standards were mixed with PE powder (10%, 25% and 40% mass ratios) and pressed into slices (diameter of 13 mm; thickness of 0.65 mm) with a tablet machine (HY-12, Tianjin Tianguang Optical Instrument Co. Ltd., China) under a pressure of 10 MPa for 2 min. To obtain the calibration curves for quantitative analysis, a series of slices with varying contents of L-histidine and α-lactose were prepared as follows: weighing different amounts of L-histidine/α-lactose, adding proper PE amounts to make their total masses 200 mg, and compressing these mixtures into series of slices with the two chemical contents ranging from 5% to 50% (5%, 10%, 15%, 20%, 25%, 30%, 40% and 50% mass ratios). Every gradient had three parallels; meanwhile, all of the samples were detected in triplicate. PE power was chosen for the tabling process because of its high transparency to THz radiation, low interference from features and easy formation of slices [30,31].

Cornstarch powders, often used as the major ingredient in dietary supplements, were chosen as additive ingredients in this study. L-histidine and α-lactose with proper amounts of cornstarch powder added were also prepared using the above tabling method. Moreover, commercial dietary supplements A and B were directly detected by THz-FDS to obtain the THz fingerprint spectra for the quantitative analysis of L-histidine and α-lactose.

2.3. Experimental setup

THz spectra were recorded by a commercial THz-FDS (TeraScan 1550, Toptica Photonics, Germany), and the schematic of the continuous wave (cw) THz spectrometer system is shown in Fig. 1. Two laser beams with adjacent frequencies generated by two distributed feedback (DFB) lasers are delivered by optical fiber and mixed in the antenna (THz emitter). Due to the effect of optical heterodyning, a continuous THz wave is radiated, and its wavelength could be controlled by changing the wavelengths of these two DFB lasers. In our system, the wavelength of the DFB laser ranged from 1533 to 1538 nm, and the frequency of the radiated THz wave ranged from 0 to 1.2 THz. Delivered by four parabolic mirrors, the THz wave was propagated through the sample and then focused on the THz receiver. The absorption spectra were recorded by DLC smart and shown on the computer.

In this study, a measurement frequency of 40 MHz was chosen as a compromise between spectral acquisition time, accuracy and resolution. Air was chosen as the reference, the humidity was kept below 20.0%, and the temperature was maintained at approximately 20 °C in all experiments.

Owing to the continuous terahertz radiation and flexible choice of the scanning frequency in THz-FDS, the spectra of samples in the range from 0.45 to 0.90 THz in the PLSR model and 0.73–0.82 THz (L-histidine)/0.45–0.61 THz (α-lactose) in the LLSR model were selected as the calibration set for rapid qualitative and quantitative analysis. Each sample was repeatedly measured three times to reduce the random error, and the average spectral data were used for further analysis. Since the original spectra were based on frequency domain information in the THz-FDS system, transmittances of the samples could be directly extracted, and then used for calculation model building and data analysis.

2.4. IC and HPLC analysis

IC and HPLC methods for the analysis of L-histidine and α-lactose in dietary supplements were applied as reference methods (Chinese GB 5009.8–2016 and GB 5009.124-2016). To obtain fingerprint chromatograms of L-histidine, sulfuric acid type cationic resin and wavelength of 570 nm were chosen for detection, with the retention time of 30 min. The analysis of α-lactose was carried out using HPLC with a differential refractive index detector (Shimadzu Corp., Kyoto, Japan). Samples were analyzed with acetonitrile-water (70:30) as mobile phase and retention time of 30 min. Injection of each sample was performed in triplicate. Details of sample preparation and analysis method are described in the Supporting Information.

Table 1
Major chemical compositions of dietary supplements A and B.

Dietary supplement	Size	Major chemical compositions
A	Diameter: 13 mm; Middle thickness: 0.65 mm	L-histidine, α-lactose, starch, iron (< 1%), vitamin C (< 1%), folic acid (< 1%), and vitamin B_{12} (< 1%).
B	Diameter, 13 mm; Middle thickness, 0.40 mm	L-histidine, starch and zinc (< 1%).

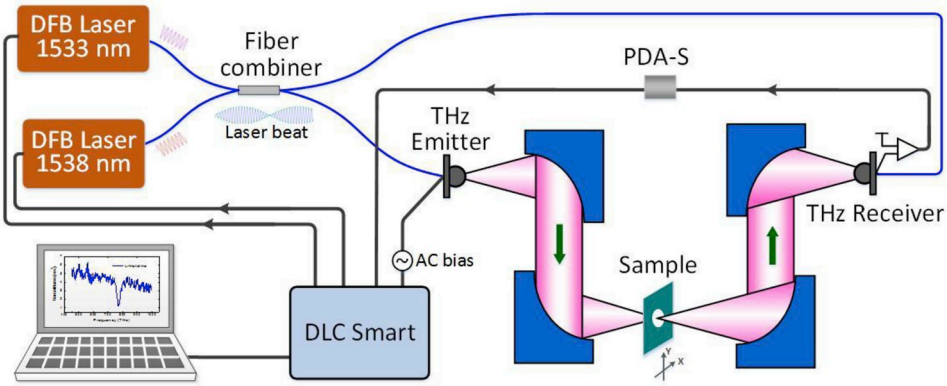

Fig. 1. Schematic of THz spectroscopy system in this experiment.

2.5. Regression modeling and evaluation

Prior to statistical analysis, the raw spectral data in this paper were smoothed using the FFT filter method through 10 smoothing points of the window. The redundancy factors of THz spectral data obtained from the signal processing system were removed by principal component analysis (PCA). Gauss and Lorentz functions were chosen as the curve-fitting algorithms for absorption peaks in this study [32]. PLSR and LLSR models were used to verify the data obtained from the experiments. The root-mean-square error of calibration (RMSEC), root-mean-square error of cross-validation (RMSECV), root-mean-square error of prediction (RMSEP) and correlation coefficient (R) values were chosen to evaluate the predictive abilities of PLSR and LLSR models [33,34].

All of the calculations in the PLSR model were carried out using TQ analyst software (version 8.3.0.125, Thermo Fisher Scientific, Inc.). Origin software (version 8.5, Origin Lab Corp.) was chosen for the fitting calculation in the LLSR model and the mapping in the whole study.

3. Results and discussion

3.1. THz spectra of L-histidine and α-lactose

The experimental transmittance spectra of L-histidine and α-lactose standards (10%, 25% and 40% weight in PE) in the range of 0.45–0.90 THz are shown in Fig. 2a and b. All of the experiments were conducted in triplicate, and the final THz spectra were averages of the three sets of data. The average RSD of three replicate measurements was less than 11% for all tested samples. As expected, both L-histidine and α-lactose exhibited their own distinctive THz spectral features. The fingerprint absorbance peaks of L-histidine and α-lactose were 0.77 THz and 0.53 THz, respectively, agreeing well with previous literature reports [35,36]. Similar to the standards, their fingerprint absorbance peaks could also be dramatically identified from the spectra of ternary mixtures containing L-histidine and α-lactose in corn starch powder (Fig. 2c) and commercial dietary supplements (Fig. 2d), indicating that their routine identification from each other in complement matrices was possible according to their spectral fingerprints. Furthermore, both extracted transmittance values of L-histidine and α-lactose were sensitive to their contents in PE matrix. The higher contents of L-histidine/α-lactose corresponded to lower transmittance signals (higher absorption values), especially in the regions adjacent to their fingerprint absorbance peaks. The peak area and peak height values also increased along with the increases in the component contents of L-histidine and α-lactose (Fig. 2a and b), which indicated that peak areas and peak heights might be recorded for analyzing these two chemicals.

3.2. Quantitative analysis

To investigate the applicability of THz-FDS for quantitative determination of L-histidine and α-lactose in dietary supplements, PLSR [37–39] and LLR models have been utilized for predicting their contents. Here, Gaussian and Lorentz fitting functions were introduced to remove the baseline of the complex matrix and to extract the absorption peak area/height data of each spectrum. As shown in Fig. 3 (a, b), higher R^2 values were obtained in Lorentz functions compared with those in Gauss functions, indicating that Lorentz functions may be more suitable for curve fitting in this study. The parameters obtained from Lorentz fitting functions are shown in Tables S1 and S2 (Supporting Information). The Lorentz fitting function F(f) at frequency f can be expressed as follows:

$$F(f) = F(f_0) + \frac{2A}{\pi}\frac{\omega}{4(f-f_c)^2+\omega^2}$$

where fc was the center frequency of the absorption peak fitted by the Lorentz curve, F(f) represented peak intensity, A was the peak area and ω was the peak width.

As shown in Fig. 3, the Lorentz fitting curves of different contents of L-histidine and α-lactose exhibited relatively good fitting results after removing the baseline. This might be attributed to the fact that the origin of the THz absorption peak is a vibrational transition as well as infrared absorption, therefore, it should follow the Lorentz model [40]. More importantly, the transmittance spectra of those samples containing different contents of L-histidine and α-lactose also presented an obvious covariation trend: that is, higher contents of chemicals correspond to lower transmittance values (Fig. 3c and d). Particular attention should be paid to the fingerprint absorbance peaks: they were more sensitive to the contents of L-histidine and α-lactose. The absorbance peak of L-histidine exhibited a relatively narrow line width, contributing to an accurate assessment of peak frequency. As shown in Fig. 3 (c, d), contents of L-histidine and α-lactose as little as 5% were observable in pellets.

Based on the spectral data acquired in the frequency range of 0.45–0.90 THz, the quantification of L-histidine and α-lactose was carried out using the PLSR model. According to the scanning frequency range of the absorbance spectra, the acquisition of each sample could be finished in 6 min. The linear fitting curves between actual concentration and calculated concentration are shown in Fig. 4 (a, b), and the corresponding fitting parameters are listed in Table 2. It is proposed that higher R values and lower RMSEC, RMSECV and RMSEP values corresponded to better prediction accuracy for the model [41]. These fitting parameters provided comparable results, indicating that both L-histidine and α-lactose could be determined by THz spectra combined

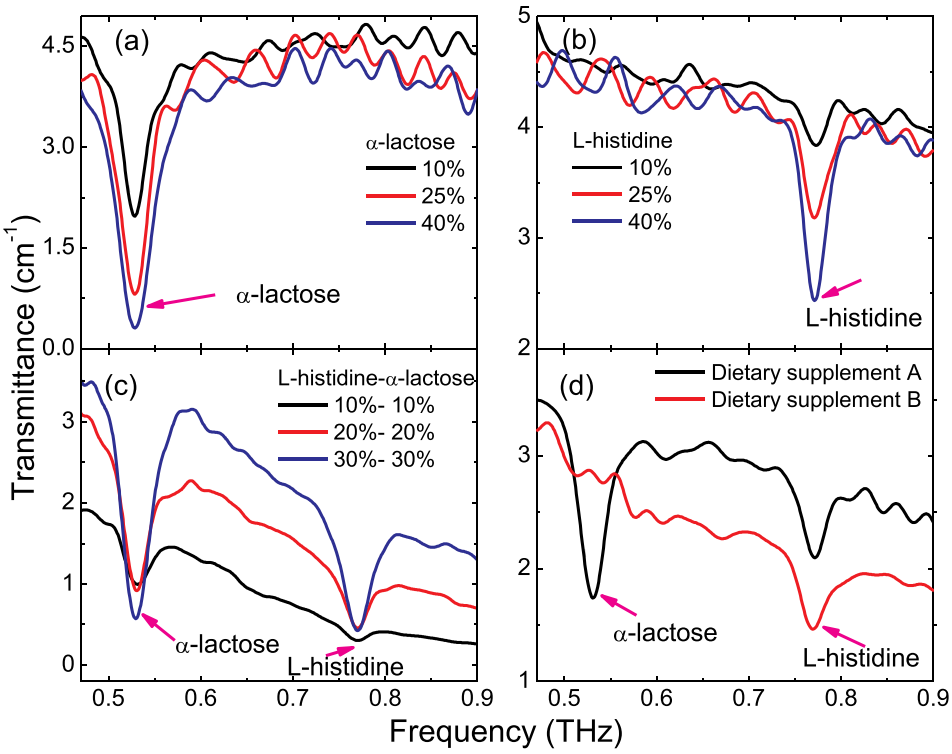

Fig. 2. THz transmittance spectra of different contents of L-histidine (a) and α-lactose (b) in PE matrix, ternary mixtures containing L-histidine and α-lactose in corn starch powder (c) and commercial dietary supplements (d). All of the original data were smoothed by FFT Filter method with 10 points of window.

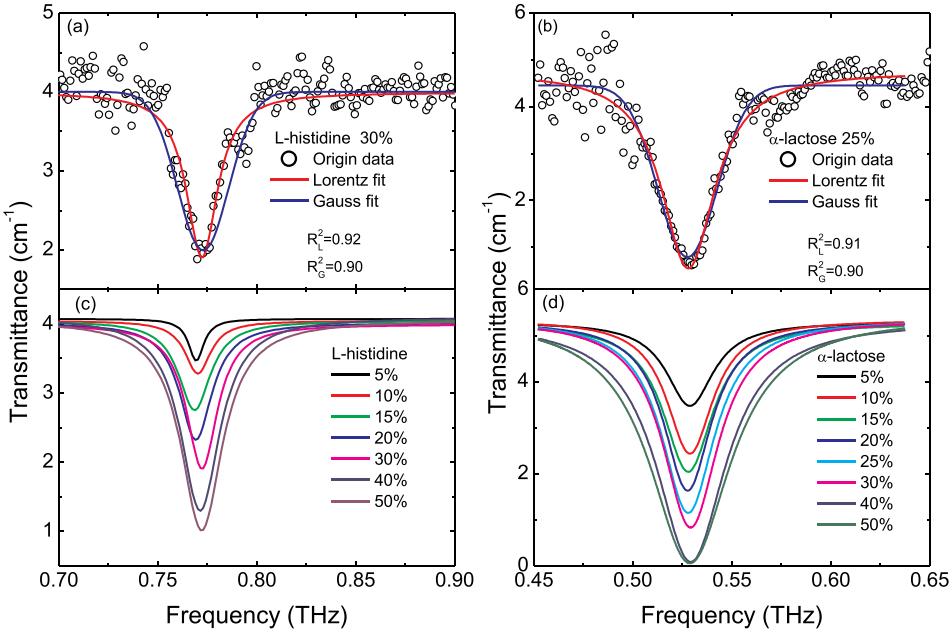

Fig. 3. Fitting curves of L-histidine with the contents of 30% (a) and α-lactose with the contents of 25% (b) fitted by Lorentz and Gauss functions, L-histidine (c) and α-lactose (d) with different contents (5%–50%) fitted by Lorentz function.

with the PLSR model. Compared with α-lactose, higher R (0.9654), and lower RMSEC (0.0546), RMSECV (0.1656) and RMSEP (0.1123) values of L-histidine were obtained, indicating a higher prediction accuracy for L-histidine using THz spectra combined with the PLSR model (see Fig. 5).

LLSR models were also applied for the quantitative analysis of L-histidine and α-lactose by using their fingerprint absorption peak heights and peak areas. The linear fitting curves between actual and calculation contents are shown in Fig. 4 (c, d, e, f). Statistical parameters obtained from LLSR models are summarized in Table 2. The relatively lower R values (0.9798 for L-histidine; 0.9571 for α-lactose) of peak height models might be because peak broadening varied with content changes in the samples. The data ranging from 0.73 to 0.82 THz (L-histidine) and 0.45 to 0.61 THz (α-lactose) were chosen as the test regions for peak area models. Compared with the parameters from peak heights and from PLSR models, higher R values ($R > 0.9899$) and lower root-mean-square errors ($RMSEC < 0.0452$, $RMSECV < 0.1323$, $RMSEP < 0.1120$) were obtained in peak area models,

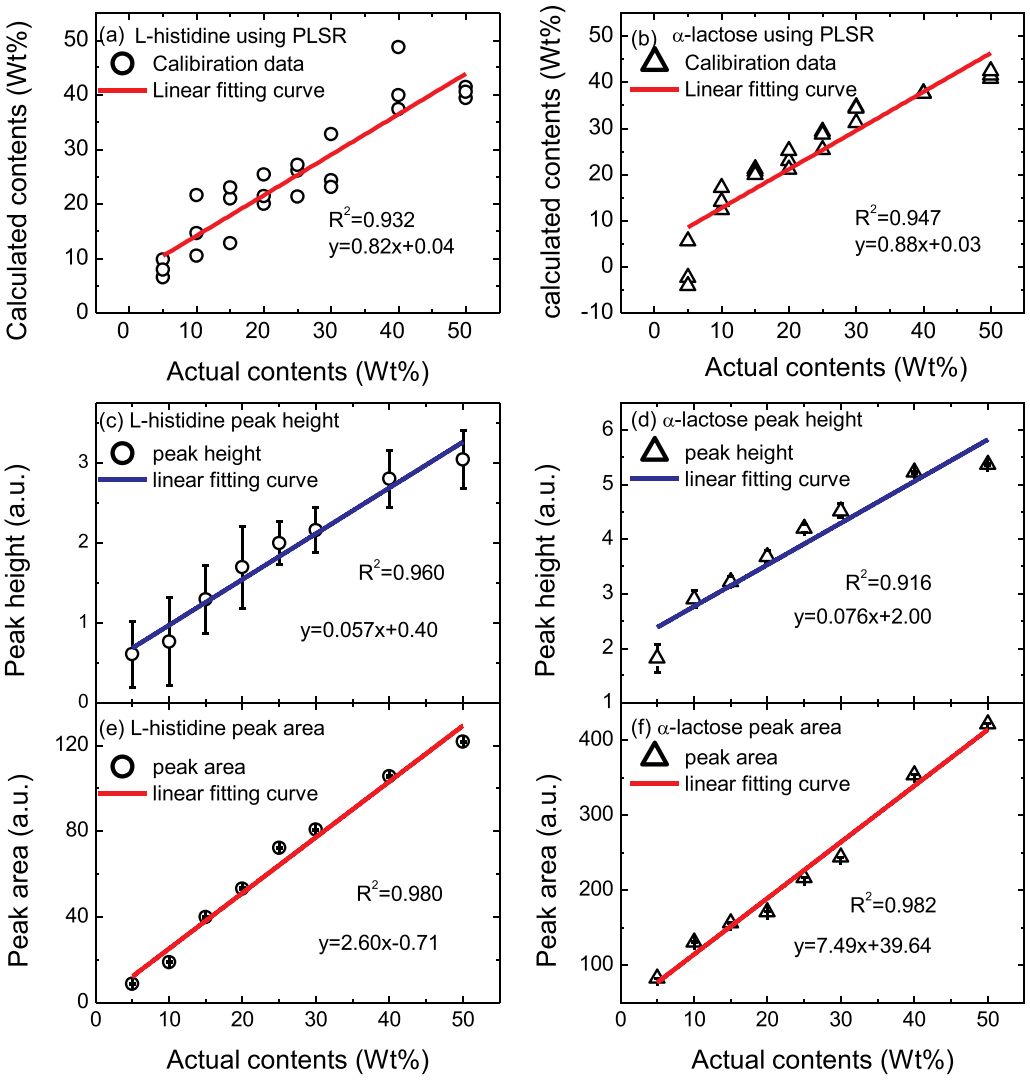

Fig. 4. Linear fitting curve between actual concentration and calculation concentration based on PLSR, LLSR by peak height and peak area (a, L-histidine based on PLSR; b, α-lactose based on PLSR; c, L-histidine based on LLSR by peak height; d, α-lactose based on LLSR by peak height; e, L-histidine based on LLSR by peak area; f, α-lactose based on LLSR by peak area).

suggesting that absorbance peak areas combined with LLSR models should be more appropriate for analyzing these two chemicals. Furthermore, the narrower THz spectrum region also corresponded to the shorter acquisition and analysis time of each spectrum. Ultimately, the acquisition time per sample could be shortened to less than 1 min.

3.3. Validation

To test the applicability of the proposed method, these two chemicals added to cornstarch matrix and their actual contents in commercial dietary supplements have been analyzed, and the results are summarized in Table 3. The transmittance spectra of L-histidine and α-lactose

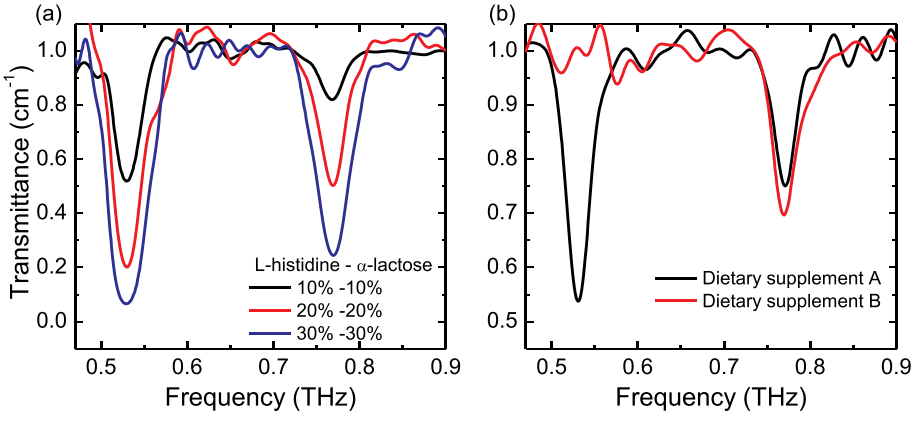

Fig. 5. THz transmittance spectra of ternary mixtures containing L-histidine and α-lactose in corn starch powder (a) and commercial dietary supplements (b) after their baselines were removed. All of the original data were smoothed by FFT Filter method with 10 points of window, and all the data for curve fitting have been processed by baseline corrections.

Table 2
The comparison of results obtained by PLSR and LLSR models for calibration and prediction.

Model	Chemicals	Spectral region (THz)	Calibration				Prediction	
			R	RMSEC	RMSECV	RMSEP	R	RMSEP
PLSR	L-histidine	0.45–0.90	0.9654	0.0546	0.1656	0.1123	0.9523	0.1059
	α-lactose	0.45–0.90	0.9731	0.0725	0.1719	0.1325	0.9522	0.1123
LLSR based on peak height	L-histidine	0.77	0.9798	0.0376	0.1421	0.0982	0.9684	0.0902
	α-lactose	0.53	0.9571	0.0412	0.1235	0.1085	0.9256	0.1020
LLSR based on peak area	L-histidine	0.73–0.82	0.9899	0.0452	0.1245	0.1120	0.9942	0.0892
	α-lactose	0.45–0.61	0.9910	0.0423	0.1323	0.1045	0.9945	0.0885

Table 3
PLSR, LLSR based on peak area and peak height results, IC/HPLC results and accuracy (%) for L-histidine and α-lactose in corn starch and dietary supplements.

Analyte	Samples	National Standard		PLSR		LLSR-peak height		LLSR-peak area	
		IC	HPLC	C (%), n = 3	A (%)	C (%), n = 3	A (%)	C (%), n = 3	A (%)
		C (%), n = 3							
L-histidine	1	10.0 ± 0.012	/	11.0 ± 0.014	110.0	12.0 ± 0.008	120.0	11.0 ± 0.010	110.0
	2	20.0 ± 0.025	/	18.0 ± 0.012	90.0	17.0 ± 0.013	85.0	19.0 ± 0.012	95.0
	3	30.0 ± 0.021	/	30.0 ± 0.029	100	27.0 ± 0.022	90.0	29.0 ± 0.018	96.7
	4	11.6 ± 0.019	/	10.0 ± 0.017	86.2	14.0 ± 0.019	120.7	11.0 ± 0.010	94.8
	5	13.3 ± 0.013	/	11.0 ± 0.021	82.7	15.0 ± 0.011	112.8	13.0 ± 0.011	97.7
α-lactose	1	/	10.0 ± 0.014	12.0 ± 0.018	120.0	11.0 ± 0.015	110.0	11.0 ± 0.017	110.0
	2	/	20.0 ± 0.016	21.0 ± 0.017	105.0	18.0 ± 0.012	90.0	22.0 ± 0.019	110.0
	3	/	30.0 ± 0.014	29.0 ± 0.019	96.7	28.0 ± 0.019	93.3	31.0 ± 0.029	103.3
	4	/	28.3 ± 0.019	29.0 ± 0.025	102.5	25.0 ± 0.018	88.3	28.0 ± 0.026	98.9
	5	/	ND	ND	/	ND	/	ND	/

C, Contents (%); A, accuracy (%); ND, not detected; Samples 1, 2, 3, 4, and 5 were corn starch 1, corn starch 2, corn starch 3, dietary supplement A and dietary supplement B, respectively.

standards added to cornstarch (Fig. S1, Supporting Information) and commercial dietary supplements were similar to those in PE matrices, as shown in Fig. 2. Owing to the interference of complex chemical compositions in food matrices such as starch, iron, vitamin C, folic acid and vitamin B12, values of baselines in their transmittance spectra were much larger than those in PE matrices, as depicted in Fig. 2 (c, d). Nevertheless, the fingerprint absorbance peaks of 0.77 THz for L-histidine and 0.53 THz for α-lactose could be significantly identified. In addition, after baselines were removed, the interferences of food matrices were largely eliminated. The absorption peak signals of L-histidine and α-lactose in complex food matrices were slightly lower than those in PE matrices, which might be attributed to the interference from the background or noise [23]. The relative data of transmittance spectra were extracted for validation of this proposed method.

To verify the accuracy of the proposed method, IC and HPLC reference methods have been performed and compared, as shown in Figs. S2, S3, S4 and S5 (Supporting Information). For L-histidine, peak areas of standards in the IC chromatogram were extracted to calculate the contents of L-histidine, with RSD less than 7%. In the HPLC method, calibration curves were constructed by plotting peak areas against the contents (R value of 0.9999). According to the research of Yu et al. [42], the accuracy was defined as follows:

$$A = \frac{\overline{C_1}}{\overline{C_2}} \times 100\%$$

where A was accuracy, $\overline{C_1}$ was the mean of measurement concentration, and $\overline{C_2}$ was the mean of HPLC/IC concentration. As shown in Table 3, the contents predicted by the LLSR model based on peak areas showed comparable data to those obtained by IC and HPLC. The accuracies were 94.8–110% and 98.9–110% for L-histidine and α-lactose, respectively. The low relative standard deviations (RSDs, 9.1%, 6.3%, 6.2%, 9.1%, 8.5% for L-histidine; 15.4%, 8.6%, 9.3%, 9.2% for α-lactose) indicated great reproducibility of this method. According to the document "A Food Labeling Guide and Guidance for Industry" suggested by the U.S. Food and Drug Administration [43], the relative error of the prediction results should be mandatorily controlled to within 20%. It could be deduced that the prediction accuracy and reproducibility could satisfy the mandatory requirement and present comparable results to those reported by Yu et al. [42] and Chen et al. [44].

In addition, the analysis time could be shortened to less than 1 min, much lower than that of either IC or HPLC (30 min). Nevertheless, ~1 min per analysis was actually too long for typical production lines. Here, the analysis time was related to the setting parameters of the instrument. When the integration time of data collection was set to be small enough, tablet detection times could be shortened to satisfy the requirements of typical production lines. However, the accuracy decreased with decreasing analysis time. The work reported here is just a preliminary study, and further study will be required to improve the precision and decrease the analysis time. In all, LLSR models combined with absorption peak areas should represent a valid method for routine analysis of L-histidine and α-lactose in complex matrices. Nevertheless, analysis of only two kinds of genuine commercial dietary supplements remains insufficient. More samples and experimental data are required for the actual application of this method.

4. Conclusions

In summary, a rapid and *in situ* quantitative analysis method based on THz fingerprint absorption peaks has been developed for L-histidine and α-lactose detection in dietary supplements. On the basis of their distinct absorption peaks, these two chemicals could be easily discriminated from each other in dietary supplements. LLSR models combined with absorption peak areas presented excellent performances for the routine analysis of L-histidine and α-lactose. Combined with the

greatly shortened acquisition time (< 1 min), the proposed method exhibited great potential for rapid and *in situ* analysis to support the oversight of food quality and to guarantee food safety.

Declaration of competing interest

The authors declare that they have no conflicts of interest in this work.

Acknowledgments

This research was supported by the China Postdoctoral Science Foundation (2017M622301) and the National Natural Science Foundation of China (Grant Nos. 21607161 and 21707148).

Appendix A. Supplementary data

Supplementary data to this article can be found online at https://doi.org/10.1016/j.talanta.2019.120469.

References

[1] K.L. Wolfe, R.H. Liu, Cellular antioxidant activity (CAA) assay for assessing antioxidants, foods, and dietary supplements, J. Agric. Food Chem. 55 (2007) 8896–8907.
[2] S.R. Karunathilaka, S.H. Choi, M.M. Mossoba, B.J. Yakes, L. Bruckner, Z. Ellsworth, C.T. Srigley, Rapid classification and quantification of marine oil omega-3 supplements using ATR-FTIR, FT-NIR and chemometrics, J. Food Compos. Anal. 77 (2019) 9–19.
[3] B. Egan, C. Hodgkins, R. Shepherd, L. Timotijevic, M. Raats, An overview of consumer attitudes and beliefs about plant food supplements, Food Funct 2 (2011) 747–752.
[4] M. Ekor, The growing use of herbal medicines: issues relating to adverse reactions and challenges in monitoring safety, Front. Pharmacol. 4 (2014) 1–10.
[5] A. Walkowiak, Ł. Ledziński, M. Zapadka, B. Kupcewicz, Detection of adulterants in dietary supplements with Ginkgo biloba extract by attenuated total reflectance Fourier transform infrared spectroscopy and multivariate methods PLS-DA and PCA, Spectrochim. Acta 208 (2019) 222–228.
[6] M.S. Blanco Canalis, A.E. Leon, P.D. Ribotta, Incorporation of dietary fiber on the cookie dough. Effects on thermal properties and water availability, Food Chem. 271 (2019) 309–317.
[7] T.D. Nguyen, M.H. Nguyen, M.T. Vu, H.A. Duong, H.V. Pham, T.D. Mai, Dual-channeled capillary electrophoresis coupled with contactless conductivity detection for rapid determination of choline and taurine in energy drinks and dietary supplements, Talanta 193 (2019) 168–175.
[8] S.H. Lu, B.Q. Li, H.L. Zhai, X. Zhang, Z.Y. Zhang, An effective approach to quantitative analysis of ternary amino acids in foxtail millet substrate based on terahertz spectroscopy, Food Chem. 246 (2017) 220–227.
[9] G.V.V. Liyanaarachchi, K.R.R. Mahanama, H.P.P.S. Somasiri, P.A.N. Punyasiri, Validation of a reversed-phase high-performance liquid chromatographic method for the determination of free amino acids in rice using L-theanine as the internal standard, Food Chem. 240 (2018) 196–203.
[10] T.H. Nguyen, A. Giri, T. Ohshima, A rapid HPLC post-column reaction analysis for the quantification of ergothioneine in edible mushrooms and in animals fed a diet supplemented with extracts from the processing waste of cultivated mushrooms, Food Chem. 133 (2012) 585–591.
[11] Y. Chen, Z.C. Tu, H. Wang, G.X. Liu, Z.W. Liao, L. Zhang, LC-Orbitrap MS analysis of the glycation modification effects of ovalbumin during freeze-drying with three reducing sugar additives, Food Chem. 268 (2018) 171–178.
[12] W. Li, X. Wu, X. Yuan, W. Zhou, T. Wu, Rapid evaluation of gamma-aminobutyric acid in foodstuffs by direct real-time mass spectrometry, Food Chem. 277 (2019) 617–623.
[13] Y. Du, J. Xue, Q. Cai, Q. Zhang, Spectroscopic investigation on structure and pH dependent Cocrystal formation between gamma-aminobutyric acid and benzoic acid, Spectrochim. Acta 191 (2018) 377–381.
[14] G. Valora, G. Munzi, R.P. Bonomo, Ternary copper(II) complexes with 1,10-phenanthroline and various aminoacidates: a spectroscopic and voltammetric study in aqueous solution, J. Inorg. Biochem. 191 (2018) 40–48.
[15] L.K. Hearn, P.P. Subedi, Determining levels of steviol glycosides in the leaves of Stevia rebaudiana by near infrared reflectance spectroscopy, J. Food Compos. Anal. 22 (2009) 165–168.
[16] J. Qin, L. Xie, Y. Ying, Feasibility of terahertz time-domain spectroscopy to detect tetracyclines hydrochloride in infant milk powder, Anal. Chem. 86 (2014) 11750–11757.
[17] S. Sommer, M. Koch, A. Adams, Terahertz time-domain spectroscopy of plasticized poly(vinyl chloride), Anal. Chem. 90 (2018) 2409–2413.
[18] C.T. Nemes, J.R. Swierk, C.A. Schmuttenmaer, A terahertz-transparent electrochemical cell for in situ terahertz spectroelectrochemistry, Anal. Chem. 90 (2018) 4389–4396.
[19] C.M. Mcgoverin, T. Rades, K.C. Gordon, Recent pharmaceutical applications of Raman and terahertz spectroscopies, J. Pharm. Sci-us 97 (2008) 4598–4621.
[20] Y. Sun, P. Du, X. Lu, P. Xie, Z. Qian, S. Fan, Z. Zhu, Quantitative characterization of bovine serum albumin thin-films using terahertz spectroscopy and machine learning methods, Biomed. Opt. Express 9 (2018) 2917–2929.
[21] M.M. Nazarov, O.P. Cherkasova, A.P. Shkurinov, A comprehensive study of albumin solutions in the extended terahertz frequency range, J. Infrared Millim. Te. 39 (2018) 840–853.
[22] C. Wang, R. Zhou, Y. Huang, L. Xie, Y. Ying, Terahertz spectroscopic imaging with discriminant analysis for detecting foreign materials among sausages, Food Control 97 (2019) 100–104.
[23] Z. Chen, Z. Zhang, R. Zhu, Y. Xiang, Y. Yang, P.B. Harrington, Application of terahertz time-domain spectroscopy combined with chemometrics to quantitative analysis of imidacloprid in rice samples, J. Quant. Spectrosc. Ra. 167 (2015) 1–9.
[24] Y. Wang, Q. Wang, Z. Zhao, A. Liu, Y. Tian, J. Qin, Rapid qualitative and quantitative analysis of chlortetracycline hydrochloride and tetracycline hydrochloride in environmental samples based on terahertz frequency-domain spectroscopy, Talanta 190 (2018) 284–291.
[25] P.C. Ashworth, E. Pickwell-Mac Pherson, E. Provenzano, S.E. Pinder, A.D. Purushotham, M. Pepper, V.P. Wallace, Teraherz pulsed spectroscopy of freshly excised human breast cancer, Opt. Express 17 (2009) 12444–12454.
[26] X. Han, S. Yan, Z. Zang, D. Wei, H. Cui, C. Du, Label-free protein detection using terahertz time-domain spectroscopy, Biomed. Opt. Express 9 (2018) 994–1005.
[27] Y. Ueno, R. Rungsawang, I. Tomita, K. Ajito, Quantitative measurements of amino acids by terahertz time-domain transmission spectroscopy, Anal. Chem. 78 (2006) 5424–5428.
[28] K. Shih, P. Pitchappa, L. Jin, C. Chen, R. Singh, C. Lee, Nanofluidic terahertz metasensor for sensing in aqueous environment, Appl. Phys. Lett. 113 (2018) 071105.
[29] G. Ok, H.J. Shin, M.C. Lim, S.W. Choi, Large-scan-area sub-terahertz imaging system for nondestructive food quality inspection, Food Control 96 (2019) 383–389.
[30] H. Wu, E.J. Heilweil, A.S. Hussain, M.A. Khan, Process analytical technology (PAT): quantification approaches in terahertz spectroscopy for pharmaceutical application, Int. J. Pharm. 97 (2008) 970–984.
[31] T. Shibata, T. Mori, S. Kojima, Low-frequency vibrational properties of crystalline and glassy indomethacin probed by terahertz time-domain spectroscopy and low-frequency Raman scattering, Spectrochim. Acta 150 (2015) 207–211.
[32] T. Sasaki, T. Sakamoto, M. Otsuka, Detection of impurities in organic crystals by high-accuracy terahertz absorption spectroscopy, Anal. Chem. 90 (2018) 1677–1682.
[33] Q. Wang, Y.H. Ma, Qualitative and quantitative identification of nitrofen in terahertz region, Chemometr. Intell. Lab. 127 (2013) 43–48.
[34] H. Zhang, Z. Li, T. Chen, B. Qin, Quantitative determination of auramine o by terahertz spectroscopy with 2dcos-plsr model, Spectrochim. Acta 184 (2017) 335–341.
[35] B. Han, Z. Han, J. Qin, Y. Wang, Z. Zhao, A sensitive and selective terahertz sensor for the fingerprint detection of lactose, Talanta 192 (2019) 1–5.
[36] S. Zong, G.H. Ren, S. Li, B. Zhang, J. Zhang, W. Qi, J. Han, H. Zhao, Terahertz time-domain spectroscopy of L-histidine hydrochloride monohydrate, J. Mol. Struct. 1157 (2018) 486–491.
[37] H. Zhang, Z. Li, T. Chen, J. Liu, Discrimination of traditional herbal medicines based on terahertz spectroscopy, Optik 138 (2017) 95–102.
[38] S. Lu, X. Zhang, Z. Zhang, Y. Yang, Y. Xiang, Quantitative measurements of binary amino acids mixtures in yellow foxtail millet by terahertz time domain spectroscopy, Food Chem. 211 (2016) 494–501.
[39] J. Tan, R. Li, Z.T. Jiang, S.H. Tang, Y. Wang, Rapid and non-destructive prediction of methylxanthine and cocoa solid contents in dark chocolate by synchronous front-face fluorescence spectroscopy and PLSR, J. Food Compos. Anal. 77 (2019) 20–27.
[40] T.G. Mayerhofer, J. Popp, Quantitative evaluation of infrared absorbance spectra - Lorentz profile versus Lorentz oscillator, ChemPhysChem 20 (2019) 31–36.
[41] H.Q. Yang, B.Y. Kuang, A.M. Mouazen, Size estimation of tomato fruits based on spectroscopic analysis, Adv. Mater. Res. 225–226 (2011) 1254–1257.
[42] M. Yu, R. Wen, L. Jiang, S. Huang, Z. Fang, B. Chen, L. Wang, Rapid analysis of benzoic acid and vitamin C in beverages by paper spray mass Spectrometry, Food Chem. 268 (2018) 411–415.
[43] FDA, Labeling and nutrition - guidance for industry: a food labeling guide, Available from: https://www.fda.gov/food/guidanceregulation/guidancedocumentsregulatoryinformation/labelingnutrition/ucm2006828.htm.
[44] D. Chen, Y. Li, Z. Tan, Z. Huang, J. Zong, Q. Li, On-line monitoring of key nutrients in yoghurt samples using digitally labelled Raman spectroscopy, Int. Dairy J. 96 (2019) 132–137.